IEEE Access
Multidisciplinary | Rapid Review | Open Access Journal

Received February 26, 2020, accepted March 15, 2020, date of publication March 19, 2020, date of current version March 31, 2020.

Digital Object Identifier 10.1109/ACCESS.2020.2981957

Range-Doppler Domain-Based DOA Estimation Method for FM-Band Passive Bistatic Radar

GEUN-HO PARK, YOUNG-KWANG SEO, AND HYOUNG-NAM KIM, (Member, IEEE)
Department of Electronics Engineering, Pusan National University, Busan 46241, South Korea

Corresponding author: Hyoung-Nam Kim (hnkim@pusan.ac.kr)

This work was supported by the Basic Science Research Program of the National Research Foundation of Korea (NRF), Ministry of Education, under Grant 2017R1D1A1B04035230.

ABSTRACT Recently, a range-Doppler map-based direction-of-arrival (DOA) estimation method was proposed for amplitude modulation (AM) radio-based passive bistatic radar (PBR). This method estimates the incident angle from the phase difference of the range-Doppler-bin (RD-bin) for the specific bistatic range of the cross-ambiguity function (CAF) and the Doppler frequency value rather than the phase difference between each antenna signal. In particular, in AM radio-based PBR, the RD-bin-based signal processing technique was adequately used to transform the range dimension of the CAF into an angular dimension. In this study, we improve the RD-bin–based DOA estimation method for frequency modulation (FM) radio-based PBR. The two main contributions of this paper are as follows. First, we present a criterion for deciding on the number of RD-bins using theoretical analysis. Second, we suggest that other target signals may become interference signals in the presence of multiple targets, which may degrade the DOA estimation accuracy. We also propose a least-squares-based algorithm to solve this problem. From the simulation results, we show that the proposed criterion for deciding on the number of RD-bins is appropriate for FM radio-based PBR and that the proposed least-squares algorithm successfully removes the target interferences.

INDEX TERMS Direction of arrival estimation, frequency modulation, interference cancellation, passive radar, array signal processing.

I. INTRODUCTION

A. BRIEF INTRODUCTION OF PASSIVE BISTATIC RADAR

Passive bistatic radar (PBR) is a passive radar system for localizing fast-moving targets by exploiting multiple illuminators of opportunity (IoO). Such IoOs were originally designed for broadcasting and communications. For example, PBR has used frequency modulation (FM) radio [1]–[4], amplitude modulation (AM) radio [5], digital television [6]–[9], digital audio broadcasting [10], global systems for mobile communications [11], [12], Wi-Fi [13], and satellite signals [14].

Among these IoOs, FM radio transmitters have been widely exploited because of their practical transmitting power (i.e., a few kilowatts). In addition, FM radio transmitters have carrier frequencies within the very high frequency (VHF) band, which is 88-108 MHz, lower than those of monostatic conventional radar systems using L, S, C, X, Ku, and Ka bands. This difference makes it possible to detect stealthy targets because stealth aircraft are known to only be able to avoid radio propagation in the frequency bands used by conventional radar systems [15].

FM radio-based PBR generally exploits a multistatic configuration, which is composed of one receiver and more than three FM transmitters. From each receiver-transmitter pair, we can estimate the time difference between a target-reflected signal and a line-of-sight (LOS) signal, also referred to as a reference signal, propagating the receiver-transmitter baseline. This time difference measurement can be transformed to bistatic range measurement. PBR can represent the target location as multiple ellipsoids whose foci are the locations of the receiver and the multiple transmitters using bistatic range measurements and transmitter-target-receiver distances. From an intersection point of these ellipsoids, the target location can be extracted as a point in three-dimensional (3D) space.

B. MOTIVATION BEHIND THIS STUDY

There needs to be more than three transmitter-receiver pairs for unambiguous target localization. However, due to the topographic conditions of the receiver location, it may be challenging to obtain all of the target detection

The associate editor coordinating the review of this manuscript and approving it for publication was Liangtian Wan.

results from multiple transmitter-receiver pairs. If one of the transmitter-receiver pairs cannot provide a sufficient signal-to-noise ratio (SNR) of the reference signal and the target signal, it may be difficult to perform target localization. In particular, mountainous terrain makes it difficult to obtain multiple measurements simultaneously.

One way to solve this problem is to obtain the target direction, i.e., the direction-of-arrival (DOA) of the target using a phased antenna array configuration. The target direction can provide the target location unambiguously, even using only one transmitter-receiver pair, because the estimate of the incident angle indicates the target location as a line. This method also improves the performance of target localization in the target-tracking process. Therefore, it is essential to estimate the DOA of a target, particularly in mountainous or urban areas.

Conventional, well-known DOA estimation algorithms, such as Bartlett [16], Capon [17], multiple signal classification (MUSIC) [18], root-MUSIC [19], estimation of signal parameters via a rotational invariance technique (ESPRIT) [20], min-norm [21], and the recent variants of these algorithms [22]–[27], have been applied in the area of passive radar [28]–[33]. However, most of these estimation algorithms are not appropriate for SNR values smaller than 0 dB because the estimation accuracy of these algorithms becomes dramatically degraded in the low SNR region (e.g., SNRs below -30 dB). The reason why we consider the low SNR region in PBR is to both improve the detection range and secure the possibility of target localization. Most FM radio-based PBRs can achieve a certain level of the detection probability even below -30 dB SNRs by increasing the processing gain in the range-Doppler (RD) map. If the DOA estimation accuracy is secured in the low SNR region, it is possible to deduce the target location as a point. Specifically, as the detection result in the RD map only gives the bistatic range and velocity information, we have tried to accurately estimate the DOAs of target signals to derive the target location, even using only a bistatic configuration. To this end, we have attempted to determine the incident angle in the low SNR region.

It is known that the Cramér-Rao bounds with unknown and known signal waveforms have significant differences mainly in the low SNR region (see [34] in Chapter 8), and the conventional algorithms are based on the assumption that the source signal is unknown. Therefore, traditional algorithms may have much higher estimation errors, particularly in the low SNR region, compared to those of other algorithms using the source signal information. Our simulation results also show the difference between the two types of DOA estimation algorithms.

Furthermore, Capon and MUSIC have limited degrees-of-freedom (DOFs), which limits the resolvable number of signals. This problem is particularly significant for FM-based passive radar. Due to the low carrier frequency of IoOs with this approach, it is not easy to establish more than tens of antennas in a restricted space. In other words, the number of resolvable target signals for DOA estimation is limited to the number of antennas when we use DOA algorithms such as Bartlett, Capon, and MUSIC.

C. RELATED WORK

As previously mentioned, the conventional DOA estimation methods have been used for finding target direction in passive radar systems. In [29], the angles of arrival were estimated by applying the ESPRIT algorithm under a semi-urban digital video broadcasting–terrestrial (DVB-T) passive radar scenario. Most of the works reported in the literature have applied the MUSIC algorithm for bearing estimation of target signals [30]. A maximum-likelihood (ML) estimator for multiband-based PBR configurations was also proposed in [31], [32]; however, it is not directly applicable to practical implementation due to its underlying assumption that the delay and Doppler frequency of the target signal are known. A beam space transformation-based DOA estimation scheme was derived in [35], and three different DOA estimation methods were considered: Capon, Taylor, and a modified Bucci algorithm; however, this system also does not utilize any information about the reference signal.

Some of the literature is limited to a particular configuration of the antenna array. A four-element Adcock antenna array-based DOA estimation method was suggested in [36], [37]. A DOA estimation algorithm for a five-element circular array was proposed in [36]. Thus, the DOA estimation algorithms in [36], [36], [37] are strictly limited to specific antenna configurations.

Many studies have presented RD map-based DOA estimation methods [5], [6], [12], [33], [35], [38]–[40]. The passive radar systems in these studies showed that range-Doppler processing is performed by correlating the reference signal with the signal received at the array of antennas. In particular, a DOA estimation algorithm using the phase information of range-Doppler bins (RD-bins) derived from two antennas was proposed [33]. However, this method is also limited, in this case, to only a two-antenna array configuration.

The DOA estimation method was also applied in an AM radio-based passive radar [5]. As an AM radio signal has a much narrower instantaneous bandwidth (10 kHz) than an FM radio signal (200 kHz), it is not easy to resolve numerous targets in the bistatic range domain. Nonetheless, the authors in [5] proposed a multiple RD-bin-based DOA estimation method, which can resolve targets by transforming the range-Doppler domain to the angle-Doppler domain. In this paper, we will mainly focus on the RD-bin-based DOA estimation algorithm presented in [5] for FM radio-based PBR instead of AM radio-based PBR.

D. CONTRIBUTIONS OF THE STUDY

In this paper, we consider an RD map-based DOA estimation method in PBR using FM radio-based IoOs.

We propose the following points:

- *We evaluate the theoretical performance of single RD-bin- and multiple RD-bin-based DOA*

estimation methods. We provide a theoretical analysis of the steering vector estimation process by comparing the input and output SNR of the steering vector estimation results and present the appropriate method to estimate the steering vector in FM radio-based PBR.

- *In the case of using the single RD-bin-based DOA estimation method, we show that one target signal component on the cross-ambiguity function (CAF) may become an interference signal to other target signals. To solve this problem, we propose an interference cancellation method that is based on the least-squares approach.*
- *The proposed method removes the target interferences by using the steering vector estimate, and it may cause SNR loss of the target component of interest. Thus, we explicitly derive the SNR loss of the target interference cancellation method based on a two-target case.*

E. OUTLINE

The rest of this paper is organized as follows. The signal model of the received signal for the range-Doppler map-based DOA estimation is presented in section II. In section III, the theoretical performance analysis of single RD-bin- and multiple RD-bin-based DOA estimation is derived. In section IV, the target interference cancellation method is proposed, and the theoretical analysis of SNR loss is described. The numerical results are detailed in section V, and conclusions are given in section VI.

F. NOTATIONS

Throughout the paper, the following notations are used. The superscript $(\cdot)^T$ denotes the transpose operator of a matrix; $(\cdot)^H$ stands for the Hermitian transpose of a matrix; $(\cdot)^*$ denotes the conjugate operator of a matrix, or a constant value; $\mathbb{C}^{n\times m}$ and $\mathbb{R}^{n\times m}$ denote a set of $n \times m$ complex-valued matrices and a set of $n \times m$ real-valued matrices, respectively; and $E[\cdot]$ stands for an expected value of a random variable or a random process.

II. RANGE-DOPPLER MAP-BASED DOA ESTIMATION

In this section, we describe the received signal model of the target signals. Consider an FM radio transmitter, a receiver antenna array with M omnidirectional antennas and N targets. It is assumed that the target signals and the reference signal are perfectly separated using beamforming techniques and interference cancellation algorithms (see [41]–[43]). Then, the received signal $\mathbf{x}(k) = [x_0(k), x_1(k), \ldots, x_{M-1}(k)]^T$ can be written as

$$\mathbf{x}(k) = \sum_{i=0}^{N-1} \eta_i \mathbf{a}(\theta_i, \phi_i) s_i(k) + \mathbf{v}(k), \quad k = 0, 1, \ldots, K-1, \tag{1}$$

where η_i denotes the complex amplitude of the ith target, $\mathbf{a}(\theta_i, \phi_i) \in \mathbb{C}^{M\times 1}$ is the steering vector with target elevation θ_i and azimuth ϕ_i, $s_i(k) = s(k-\tau_i)e^{j2\pi\nu_i k}$ is the ith target echo signal, and $\mathbf{v}(k) \in \mathbb{C}^{M\times 1}$ denotes a spatially white Gaussian noise process. In our received signal model, we assume that the received signals of each antenna are synchronized using various calibration techniques [44], [45]. As the SNR of the reference signal is much higher than that of the target echoes, the reference signal $x_r(k)$ can be written as $x_r(k) \approx s(k)$.

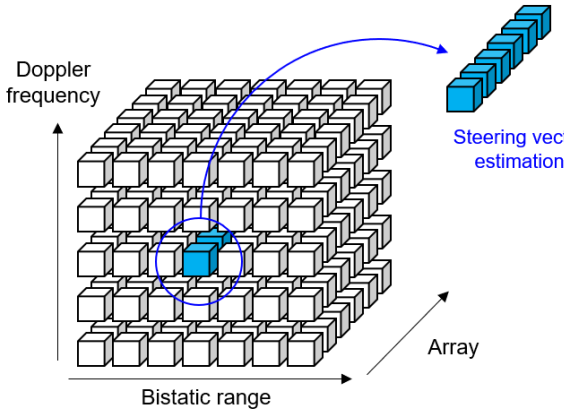

FIGURE 1. Range-Doppler-array map-based data cube.

Target detection is performed on a CAF. The received signal at the mth antenna, $x_m(k)$, $m = 0, \ldots, M-1$, and the reference signal $s(k)$ can produce the CAF of each antenna, which is defined as

$$c_m(\tau, \nu) = \sum_{k=0}^{K-1} s(k)\, x_m^*(k+\tau) e^{-j2\pi\nu k}, \tag{2}$$

where τ and ν denote the sample delay and the normalized Doppler frequency, respectively. From (2), the RD-bin $\mathbf{c}(\tau, \nu) \in \mathbb{C}^{M\times 1}$ in the range-Doppler domain is represented as:

$$\mathbf{c}(\tau, \nu) = [c_0(\tau, \nu), c_1(\tau, \nu), \ldots, c_{M-1}(\tau, \nu)]^T. \tag{3}$$

The RD-bin $\mathbf{c}(\tau, \nu)$ is our main concern in this study, and it can be viewed as a data cube or a multidimensional array, as shown in Fig. 1. As shown in this figure, the steering vector $\mathbf{a}(\theta, \phi)$ can be estimated from the RD-bin $\mathbf{c}(\tau, \nu)$. To show this, the RD-bin $\mathbf{c}(\tau, \nu)$ can be also derived in vector form using (1) and written as:

$$\mathbf{c}(\tau, \nu) = \sum_{k=0}^{K-1} s(k)\mathbf{x}^*(k+\tau) e^{-j2\pi\nu k}. \tag{4}$$

Substituting (1) into (4), we obtain

$$\mathbf{c}(\tau, \nu) = \sum_{i=0}^{N-1} \eta_i^* A(\tau - \tau_i, \nu - \nu_i)\mathbf{a}_i^* + \sum_{k=0}^{K-1} s(k)\mathbf{v}^*(k+\tau) e^{-j2\pi\nu k}, \tag{5}$$

where $A(\tau, \nu)$ denotes the ambiguity function of $s(k)$ and $\mathbf{a}_i$ is a simplified notation for $\mathbf{a}(\theta_i, \phi_i)$. The ambiguity function $A(\tau, \nu)$ is defined as:

$$A(\tau, \nu) = \sum_{k=0}^{K-1} s(k)s^*(k+\tau) e^{-j2\pi\nu k}. \tag{6}$$

If the target signals are assumed to be uncorrelated with each other, then the RD-bin for $\tau = \tau_i$ and $\nu = \nu_i$ in (5) can be rewritten as:

$$\mathbf{c}(\tau_i, \nu_i) = \eta_i^* A(0,0)\mathbf{a}_i^* + \sum_{k=0}^{K-1} s(k)\mathbf{v}^*(k+\tau_i)e^{-j2\pi\nu_i k}, \quad (7)$$

where $A(0,0) = \sum_{k=0}^{K-1} |s(k)|^2 = K$. This equation shows that the RD-bin of $\mathbf{c}(\tau_i, \nu_i)$ can be used to obtain the steering vector estimate of $\mathbf{a}_i$. Therefore, to obtain $\mathbf{a}_i$, the target detection should be performed on the CAF in advance. A constant false alarm rate (CFAR) detector can be used to estimate the number of targets, range, and Doppler frequency measurements [46]. In this study, we assume that the number of targets N, range, and Doppler frequency measurements are known by using the CFAR detector.

If we denote an estimate of the steering vector as $\hat{\mathbf{b}}_i$, which is a function of $\mathbf{c}(\tau, \nu)$, then the spatial spectrum of the ith target is obtained from

$$P_i(\theta, \phi) = \mathbf{a}^H(\theta, \phi)\hat{\mathbf{b}}_i. \quad (8)$$

The derivation of $\hat{\mathbf{b}}_i$ will be discussed in the next subsection. The final estimate of the incident angle is followed by:

$$\{\hat{\theta}_i, \hat{\phi}_i\} = \arg\max_{\theta,\phi} |P_i(\theta, \phi)|^2, \quad i = 1, \ldots, N. \quad (9)$$

As described in [5], we can consider using other DOA estimation methods, such as the Capon and MUSIC algorithms, instead of the Bartlett method.

III. STEERING VECTOR ESTIMATION METHODS AND PERFORMANCE ANALYSIS

A. DEFINITION OF SINGLE RD-BIN- AND MULTIPLE RD-BIN-BASED DOA ESTIMATION

An estimate of the steering vector $\hat{\mathbf{b}}_i$, which is used to compute the spatial spectrum, can be derived in two ways. First, the single RD-bin can be directly selected to calculate the spatial spectrum, i.e.,

$$\hat{\mathbf{b}}_i = \mathbf{c}(\tau_i, \nu_i), \quad i = 1, \ldots, K. \quad (10)$$

As this method only depends on a single RD-bin, it is referred to as *single RD-bin-based DOA estimation* in this paper. Second, multiple RD-bins may be selected to produce the estimate $\hat{\mathbf{b}}_i$. If we consider the arithmetic mean of the multiple RD-bins, then

$$\hat{\mathbf{b}}_i = \frac{1}{L_i}\sum_{l=1}^{L_i} \mathbf{c}(\tau_i^{(l)}, \nu_i^{(l)}), \quad i = 1, \ldots, K, \quad (11)$$

where $(\tau_i^{(l)}, \nu_i^{(l)})$ is a pair element of time-delay and Doppler frequency measurement included in a set of $\mathcal{A}_i = \{(\tau_i^{(l)}, \nu_i^{(l)}), l = 1, \ldots, L_i\}$. This is derived from the multiple RD-bins; therefore, it is referred to as *multiple RD-bin-based DOA estimation* in this paper. The estimate obtained based on the multiple RD-bins may be computed in various ways.

The multiple RD-bin-based DOA estimation can be used when the CAF is as shown in Fig. 2, which is derived when the FM stereo message signal only has a 19 kHz pilot tone. If

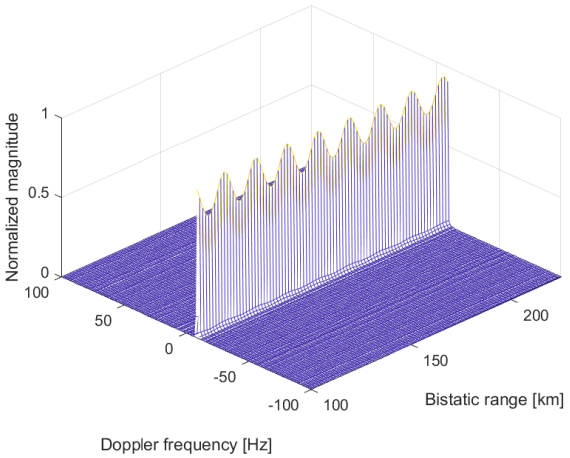

FIGURE 2. CAF of FM-radio-based PBR when the message signal includes only a 19 kHz pilot tone signal.

$A(\tau, \nu_i) \approx A(0, \nu_i)$ for all τ, as shown in Fig. 2, all RD-bins lying on a specific Doppler frequency ν_i include the steering vector component $\mathbf{a}_i$ as follows:

$$\mathbf{c}(\tau, \nu_i) = \eta_i^* A(0,0)\mathbf{a}_i^* + \sum_{k=0}^{K-1} s(k)\mathbf{v}^*(k+\tau)e^{-j2\pi\nu_i k}. \quad (12)$$

Note that (12) is distinguished from (7). Specifically, (12) is a function of τ, whereas (7) holds only for a specific τ_i and ν_i. To extract $\mathbf{a}_i$ from the multiple RD-bins of $\mathbf{c}(\tau, \nu_i)$, the arithmetic mean of all $\mathbf{c}(\tau, \nu_i)$ with respect to τ is a solution.

B. THEORETICAL PERFORMANCE ANALYSIS OF STEERING VECTOR ESTIMATION METHODS

To investigate whether or not the multiple RD-bin-based steering vector estimation has a higher SNR than that of the single RD-bin-based estimation, the SNR analysis is discussed in this subsection. The multiple RD-bin-based DOA estimation method was applied to AM radio-based PBR [5]. As the AM radio signal features a narrow instantaneous bandwidth, the transformation of a range measurement to an angle is effective for detecting multiple targets. Therefore, it may be concluded that the multiple RD-bin-based steering vector estimation and the transformation could be a solution to resolving the multiple target signals in AM-radio-based PBR.

In this paper, it would be useful to analyze the estimation accuracy of both the single RD-bin- and multiple RD-bin-based DOA estimations. As the DOA estimation error is deeply involved in the SNR of $\hat{\mathbf{b}}_i$, we derive the theoretical SNR.

1) SNR ANALYSIS OF SINGLE RD-BIN-BASED STEERING VECTOR ESTIMATION

Our objective is to derive the theoretical SNR of $\hat{\mathbf{b}}_i$. First, we consider the single RD-bin-based steering vector estimation. From (1), the received signal $\mathbf{x}(k)$ for $N = 1$ is written as:

$$\mathbf{x}(k) = \eta_0\, s(k-\tau_0)e^{-j2\pi\nu_0 k}\mathbf{a}(\theta_0, \phi_0) + \mathbf{v}(k). \quad (13)$$

Substituting (13) in (4) with some mathematical modifications, the RD-bin at the mth antenna for $\tau = \tau_0$ and $\nu = \nu_0$ can be obtained as:

$$\begin{aligned} c_m(\tau_0, \nu_0) &= \sum_{k=0}^{K-1} s(k) x_m^*(k+\tau_0) e^{-j2\pi \nu_0 k} \\ &= \eta_0^* a_m^*(\theta_0, \phi_0) A(0,0) \\ &\quad + \sum_{k=0}^{K-1} s(k) v_m^*(k+\tau_0) e^{-j2\pi \nu_0 k}, \end{aligned} \tag{14}$$

where $a_m(\theta_0, \phi_0)$ denotes the mth element of the steering vector $\mathbf{a}(\theta_0, \phi_0)$. We also assume that $E\left[|s(k)|^2\right] = 1$ in (14). As $\eta_0^*\, a_m^*(\theta_0, \phi_0) A(0,0)$ and $\sum_{k=0}^{K-1} s(k) v_m^*(k+\tau_0) e^{-j2\pi \nu_0\, k}$ represent the component contributing to the peak value and noise, respectively, the SNR of the target signal in $c_m(\tau_0, \nu_0)$ can be derived from:

$$SNR = \frac{|\eta_0|^2\, |A(0,0)|^2}{E\left[\left|\sum_{k=0}^{K-1} s(k) v_m^*(k+\tau_0) e^{-j2\pi \nu_0 k}\right|^2\right]}. \tag{15}$$

To simplify (15), the denominator in (15) can be expressed as:

$$\sum_{k_1=0}^{K-1} \sum_{k_2=0}^{K-1} E\left[s(k_1) s^*(k_2) \tilde{v}_m^*(k_1+\tau_0) \tilde{v}_m(k_2+\tau_0)\right], \tag{16}$$

where $\tilde{v}_m(k+\tau) = v_m(k+\tau) e^{-j2\pi \nu_0\, k}$. As the expectation of the noise components in (16) approaches zero for $k_1 \neq k_2$, we obtain

$$\sum_{k=0}^{K-1} E\left[|s(k)|^2\right] E\left[|v_m(k+\tau_0)|^2\right] = K P_v, \tag{17}$$

where $E\left[|v_m(k+\tau_0)|^2\right] = P_v$. Subsequently, we have

$$SNR_1 = \frac{|\eta_0|^2\, K^2}{K P_v} = \frac{|\eta_0|^2\, K}{P_v}. \tag{18}$$

This result indicates that the SNR of the single RD-bin-based steering vector estimation increases as the number of observation samples of K and the power of the target echo signal increases.

2) SNR ANALYSIS OF MULTIPLE RD-BIN-BASED STEERING VECTOR ESTIMATION

In this subsection, the theoretical SNR of the multiple RD-bin-based steering vector estimation is discussed. The derivation is similar; however, there is a difference from the single RD-bin method, particularly in the calculation of the noise variance.

If we consider the sample mean of R RD-bins at the mth antenna, $z_m(\nu)$, we have

$$\begin{aligned} z_m(\nu) &= \frac{1}{R} \sum_{r=0}^{R-1} c_m(\tau_r, \nu) \\ &= \frac{\eta_0^* a_m^*(\theta_0, \phi_0)}{R} \sum_{r=0}^{R-1} A(\tau_r - \tau_0, \nu - \nu_0) \\ &\quad + \frac{1}{R} \sum_{r=0}^{R-1} \sum_{k=0}^{K-1} s(k) v_m^*(k+\tau_r) e^{-j2\pi \nu k}. \end{aligned} \tag{19}$$

When we assume $A(\tau_r, 0) \approx A(0,0)$ for all $\tau_r \geq 0$, as shown in Fig. 2, (19) for $\nu = \nu_0$ can be rewritten as follows:

$$\begin{aligned} z_m(\nu_0) &= \eta_0^* a_m^*(\theta_0, \phi_0) A(0,0) \\ &\quad + \frac{1}{R} \sum_{r=0}^{R-1} \sum_{k=0}^{K-1} s(k) v_m^*(k+\tau_r) e^{-j2\pi \nu_0 k}. \end{aligned} \tag{20}$$

From (14) and (20), we can see that the multiple RD-bin-based steering vector estimation has a different noise component. For the calculation of the SNR, we need to simplify

$$E\left[\left|\frac{1}{R} \sum_{r=0}^{R-1} \sum_{k=0}^{K-1} s(k) v_m^*(k+r) e^{-j2\pi \nu_0 k}\right|^2\right]. \tag{21}$$

Similar to the single RD-bin case, the expectation of the noise component becomes

$$\begin{aligned} &\frac{1}{R^2} \sum_{r_1=0}^{R-1} \sum_{r_2=0}^{R-1} \sum_{k_1=0}^{K-1} \sum_{k_2=0}^{K-1} E\left[s(k_1) s^*(k_2) e^{-j2\pi \nu_0 (k_1 - k_2)}\right] \\ &\qquad \cdot E\left[v_m^*(k_1 + r_1) v_m(k_2 + r_2)\right]. \end{aligned} \tag{22}$$

As $E\left[s(k_1) s^*(k_2) e^{-j2\pi \nu_0 (k_1 - k_2)}\right] \leqq 1$, (22) has an upper bound of

$$\frac{1}{R^2} \sum_{r_1=0}^{R-1} \sum_{r_2=0}^{R-1} \sum_{k_1=0}^{K-1} \sum_{k_2=0}^{K-1} E\left[v_m^*(k_1 + r_1) v_m(k_2 + r_2)\right]. \tag{23}$$

The expectation of (23) with respect to k_1 and k_2 satisfies $E\left[v_m^*(q_1) v_m(q_2)\right] = 0$ for $q_1 \neq q_2$, where $q_m = k_m + r_m$. The simplification problem of (23) can be easily accomplished by counting the number of cases that satisfy $q_1 = q_2$ for $k_1, k_2 \in \{0, 1, \ldots, K-1\}$ and $r_1, r_2 \in \{0, 1, \ldots, R-1\}$. This problem can be solved using the following Lemma 1.

Lemma 1: The number of cases that satisfy $k_1 + r_1 = k_2 + r_2$ for $k_1, k_2 \in \{0, 1, \ldots, K-1\}$ and $r_1, r_2 \in \{0, 1, \ldots, R-1\}$ is derived by:

$$\frac{R(3KR - R^2 + 1)}{3}. \tag{24}$$

Proof: If we denote $k_2 - k_1 = \Delta k$ and $r_1 - r_2 = \Delta r$ where $\Delta k \in \{-K+1, \ldots, K-1\}$ and $\Delta r \in \{-R+1, \ldots, R-1\}$, then the number of cases satisfying $\Delta r = \Delta k$ is equivalent to $(R - |\Delta r|)(K - |\Delta r|)$ for all Δr. Therefore, the total number of the cases is equal to

$$KR + 2 \sum_{\Delta r=1}^{R-1} (R - \Delta r)(K - \Delta r), \tag{25}$$

and this is simplified as the result of Lemma 1.

Therefore, we can simplify (23) as follows:

$$\begin{cases} \dfrac{(3KR - R^2 + 1) P_v}{3R}, & q_1 = q_2, \\ 0, & q_1 \neq q_2. \end{cases} \tag{26}$$

The SNR of the multiple RD-bins at the mth antenna is readily derived as:

$$SNR_2 \leqq \frac{|\eta_0|^2 K^2}{\frac{(3KR - R^2 + 1) P_v}{3R}} = \frac{3R\, |\eta_0|^2\, K^2}{(3KR - R^2 + 1) P_v}. \tag{27}$$

The number of RD-bins, R, is significantly fewer than the observation samples, K, in FM radio-based PBR. For example, the observation time is generally 1 s, and the sampling frequency is 200 kHz; thus, $K = 200,000$. If we consider a maximum bistatic range of 300 km, then $R = 200$. The approximation in (27) using $K \gg R \gg 1$ leads to

$$SNR_2 \leqq \frac{3R\,|\eta_0|^2\,K^2}{(3KR - R^2 + 1)P_v} \approx \frac{|\eta_0|^2\,K}{P_v}. \tag{28}$$

The interesting point in the SNR analysis is that the multiple RD-bin-based steering vector estimation has an upper bound, which is the SNR of the single RD-bin case. In other words, the SNR of the multiple RD-bin-based method in (28) cannot exceed the SNR of the single RD-bin-based method (see (18)). The equality of (28) holds only for IoOs whose transmit signals have narrow instantaneous bandwidth (e.g., the silent message signal in FM-radio broadcasting). However, if the instantaneous bandwidth increases, the SNR of the multiple RD-bins may decrease because the equality of $E\left[s(k_1)s^*(k_2)e^{-j2\pi\nu_0(k_1-k_2)}\right] \leqq 1$ no longer holds.

Compared to an AM radio signal, the FM-radio signal has a much wider instantaneous bandwidth. In addition, the occurrence of the silent message signal in FM-broadcasting is not that common, and the estimation performance of the multiple RD-bin-based method would be degraded. We therefore consider and propose to use the single RD-bin-based steering vector estimation method in FM-radio-based PBR. This proposal will also be verified from the simulation results in Section V.

IV. RANGE-DOPPLER MAP-BASED DOA ESTIMATION IN THE PRESENCE OF TARGET INTERFERENCE

Consider that multiple target signals are received and assume that these are uncorrelated with each other. That is, the difference between the bistatic range and the Doppler frequency cannot be neglected, i.e., $A(\tau_0-\tau_1, \nu_0-\nu_1) \approx 0$ for $N = 2$. In this case, the RD-bins for (τ_0, ν_0) and (τ_1, ν_1) are as follows:

$$\begin{aligned}\mathbf{c}(\tau_0, \nu_0) &= \eta_0^* A(0,0)\mathbf{a}_0^* + \boldsymbol{\epsilon}(\tau_0, \nu_0),\\ \mathbf{c}(\tau_1, \nu_1) &= \eta_1^* A(0,0)\mathbf{a}_1^* + \boldsymbol{\epsilon}(\tau_1, \nu_1),\end{aligned} \tag{29}$$

where $\boldsymbol{\epsilon}(\tau_i, \nu_i)$ is defined as the noise component as follows:

$$\boldsymbol{\epsilon}(\tau_i, \nu_i) = \sum_{k=0}^{K-1} s(k)\mathbf{v}^*(k+\tau_i)e^{-j2\pi\nu_i k}. \tag{30}$$

In (29), none of the RD-bins are affected by other RD-bins.

However, if $A(\tau_i-\tau_j, \nu_i-\nu_j) \not\approx 0$, then (29) can be rewritten as

$$\begin{aligned}\mathbf{c}_0 &= \eta_0^* A_{00}\mathbf{a}_0^* + \eta_1^* A_{01}\mathbf{a}_1^* + \boldsymbol{\epsilon}_0,\\ \mathbf{c}_1 &= \eta_0^* A_{10}\mathbf{a}_0^* + \eta_1^* A_{00}\mathbf{a}_1^* + \boldsymbol{\epsilon}_1,\end{aligned} \tag{31}$$

where the notation of $\boldsymbol{\epsilon}(\tau_i, \nu_i)$ for $i = 0, 1$ is abbreviated as $\boldsymbol{\epsilon}_i$, and $A(\tau_i - \tau_j, \nu_i - \nu_j)$ is abbreviated as A_{ij}. Note that $A_{ii} = A_{jj} = K$. If $\mathbf{c}_0$ contains $\mathbf{a}_1$, then the spatial spectrum may construct an additional peak of target 2. Fig. 3 shows an example of a CAF where the two targets are closely spaced,

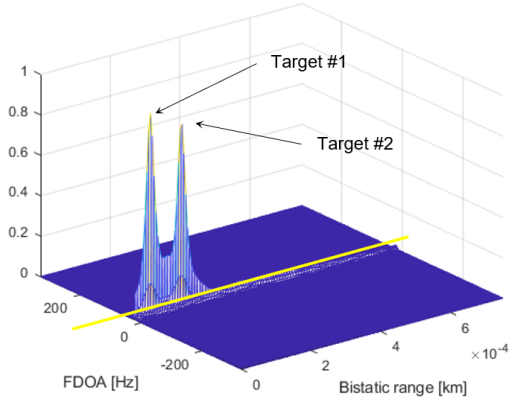

FIGURE 3. Closely spaced two-targets in CAF.

especially in the Doppler frequency dimension, and this may cause the problem of target interference.

Our objective is to remove other target components in the steering vector of interest and to extract the steering vector estimate. For example, in (31), the objective is to remove $\mathbf{a}_1$ from $\mathbf{c}_0$. Similarly, $\mathbf{a}_0$ should be removed from $\mathbf{c}_1$.

3) TARGET INTERFERENCE CANCELLATION FOR A TWO-TARGET CASE

Consider the problem of target interference cancellation with a two-target case. As previously described in (31), $\mathbf{a}_0$ and $\mathbf{a}_1$ should be extracted from $\mathbf{c}_0$ and $\mathbf{c}_1$, respectively.

The simplest way to do this is to use the weighted sum approach. The following equation would be a solution for the estimation of $\mathbf{a}_0$:

$$\begin{aligned}\tilde{\mathbf{c}}_0 = \mathbf{c}_0 - \alpha_0\mathbf{c}_1 &= \eta_0^*(A_{00} - \alpha_0 A_{10})\mathbf{a}_0^*\\ &\quad + \eta_1^*(A_{01} - \alpha_0 A_{00})\mathbf{a}_1^* + \boldsymbol{\epsilon}_0 - \alpha_0\boldsymbol{\epsilon}_1,\end{aligned} \tag{32}$$

where α_0 is a weight for interference mitigation. To remove the component of $\mathbf{a}_1$ from $\mathbf{c}_0$, we have

$$\alpha_0 = \frac{A_{01}}{A_{00}}, \tag{33}$$

and (32) can be rewritten as

$$\tilde{\mathbf{c}}_0 = \eta_0^*\left(A_{00} - \frac{A_{01}A_{10}}{A_{00}}\right)\mathbf{a}_0^* + \boldsymbol{\epsilon}_0 - \frac{A_{01}}{A_{00}}\boldsymbol{\epsilon}_1. \tag{34}$$

As we can see, the weighted sum approach can remove the component of $\mathbf{a}_1$ from $\mathbf{c}_0$. This approach can also be applied to the extraction of $\mathbf{a}_1$.

Before starting the analysis, it is crucial to know whether (33) is computable or not. Because A_{00} is the ambiguity function of the reference signal, the equation is computable. In addition, we already have the measurements of the bistatic range and the Doppler frequency of the multiple targets; thus, A_{01} and A_{10} can easily be obtained.

4) SNR LOSS OF TARGET INTERFERENCE CANCELLATION FOR TWO-TARGET CASE

As previously described, the target interference can be mitigated using (34). However, the magnitude of $\mathbf{a}_0$ would be

reduced by the weighted sum method. In this subsection, we consider the SNR loss of the target interference cancellation with a two-target case.

Let

$$\sigma_s^2 = |\eta_0|^2 \left| A_{00} - \frac{A_{01}A_{10}}{A_{00}} \right|^2 \tag{35}$$

and

$$\sigma_n^2 = E\left[\left| \epsilon_{0,m} - \alpha_0 \epsilon_{1,m} \right|^2 \right], \tag{36}$$

where $\epsilon_{i,m}$ denotes the mth entry of $\boldsymbol{\epsilon}_i$. To simplify the derivation, we only consider the mth entry of $\boldsymbol{\epsilon}_0 - \alpha_0 \boldsymbol{\epsilon}_1$, $\epsilon_{0,m}$, and $\epsilon_{1,m}$. Then, we have $SNR_{\tilde{\mathbf{c}}_0} = \sigma_s^2/\sigma_n^2$.

The first step is to derive the inequality about the squared magnitude of $\eta_0^* (A_{00} - A_{01}A_{10}/A_{00})$. Using $A_{00} = \sum_{k=0}^{K-1} |s(k)|^2 = K$ and $A_{ij} = A_{ji}^*$ for $\nu_1 = \nu_0$, we have

$$\left| \eta_0^* \left(A_{00} - \frac{A_{01}A_{10}}{A_{00}} \right) \right|^2 = |\eta_0|^2 \left(K - \frac{|A_{10}|^2}{K} \right)^2. \tag{37}$$

As $0 \leqq |A_{10}| \leqq K$, the above term is represented by the following inequality:

$$0 \leqq K - \frac{|A_{10}|^2}{K} \leqq K. \tag{38}$$

The component of the ambiguity function A_{10} is related to the range resolution and the message signal. In other words, A_{10} is a random variable in a single period of the observation time. From (38), we can see that the signal power may decrease slightly.

The second step is to compute σ_s^2, which can be derived by

$$\sigma_s^2 = K^2 |\eta_0|^2 (1 - |\alpha_0|^2). \tag{39}$$

The final step is to compute σ_n^2, which is obtained by

$$\sigma_n^2 = E[|\epsilon_{0,m}|^2 - \alpha_0^* \epsilon_{0,m} \epsilon_{1,m}^* - \alpha_0 \epsilon_{0,m}^* \epsilon_{1,m} + |\alpha_0|^2 |\epsilon_{1,m}|^2]. \tag{40}$$

As previously described in (17), we have $E\left[|\epsilon_{0,m}|^2\right] = E\left[|\epsilon_{1,m}|^2\right] = P_\nu K$, where $P_\nu = E\left[|\nu_m(k)|^2\right]$. The expectation of $\epsilon_{0,m}\epsilon_{1,m}^*$ is

$$E\left[\epsilon_{0,m}\epsilon_{1,m}^*\right] = E\left[\sum_{k_0=0}^{K-1} \sum_{k_1=0}^{K-1} s(k_0) s^*(k_1) \nu_m^*(k_0 + \tau_0) \nu_m(k_1 + \tau_1) \right]. \tag{41}$$

If $k_0 + \tau_0 \neq k_1 + \tau_1$, the term in the above summation becomes zero. As the number of cases satisfying $k_0 + \tau_0 = k_1 + \tau_1$ is $K - |\tau_0 - \tau_1|$ for $k_0, k_1 = 0, \ldots, K-1$, (41) is written as

$$E\left[\epsilon_{0,m}\epsilon_{1,m}^*\right] = \begin{cases} (K - |\tau_0 - \tau_1|)\, \alpha_0\, P_\nu, & q_0 = q_1, \\ 0, & q_0 \neq q_1, \end{cases} \tag{42}$$

and

$$E\left[\epsilon_{0,m}^*\epsilon_{1,m}\right] = \begin{cases} (K - |\tau_0 - \tau_1|)\, \alpha_0^* P_\nu, & q_0 = q_1, \\ 0, & q_0 \neq q_1, \end{cases} \tag{43}$$

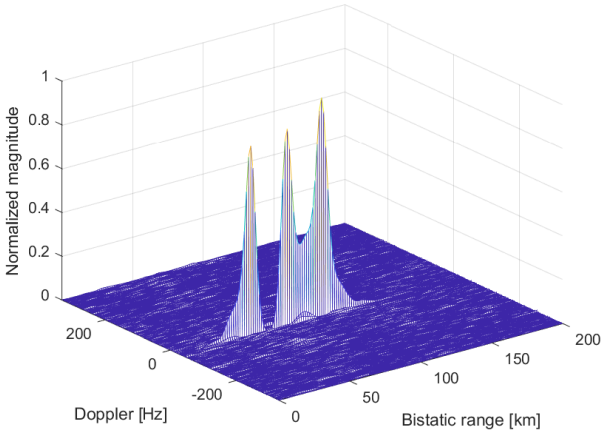

FIGURE 4. An example of CAF for three targets whose Doppler frequencies are the same.

where $q_i = k_i + \tau_i$. Then, (40) can be simplified as

$$\sigma_n^2 = K P_\nu \left(1 - |\alpha_0|^2 + \frac{2|\tau_0 - \tau_1||\alpha_0|^2}{K} \right). \tag{44}$$

By using (39) and (44), we can finally derive the SNR as follows:

$$SNR_{\tilde{\mathbf{c}}_0} = \frac{\sigma_s^2}{\sigma_n^2} = \frac{K|\eta_0|^2(1 - |\alpha_0|^2)}{P_\nu \left(1 - |\alpha_0|^2 + \frac{2|\tau_0 - \tau_1||\alpha_0|^2}{K} \right)}. \tag{45}$$

The remarkable thing in (45) is that the interference cancellation result has an almost equivalent value in (18). If $2|\tau_0 - \tau_1||\alpha_0|^2/K \approx 0$, then the SNR is expressed as

$$SNR_{\tilde{\mathbf{c}}_0} \approx \frac{K|\eta_0|^2}{P_\nu}, \tag{46}$$

which is the same as the initial value of the SNR in (18). In general, $K \gg 2|\tau_0 - \tau_1||\alpha_0|^2$ is satisfied. For example, in FM radio-based PBR, the observation samples of $K = 200,000$ are used. As $|\alpha_0|^2 \leqq 1$ and $|\tau_0 - \tau_1|$ have much smaller values than K, the approximation is reasonable. Hence, it can be concluded that the SNR loss in the example of the two-target case can be ignored.

5) GENERALIZATION OF TARGET INTERFERENCE CANCELLATION FOR A MULTITARGET CASE

Now we are ready to discuss a general problem of the existing N target case. If we have $N = 3$ targets lying on the same Doppler frequency dimension, the CAF will be represented as shown in Fig. 4. In this case, a single target is influenced by the other two targets. We may try to solve this problem using the weighted sum approach, as in the two-target case, but it is not easy to derive the solution due to its complexity.

Instead of using the weighted sum approach, the optimization method is much simpler. The proposed method is based on the following optimization problem:

$$\min_{\boldsymbol{\alpha}} ||\mathbf{x} - \mathbf{U}\boldsymbol{\alpha}||^2, \tag{47}$$

where $\boldsymbol{\alpha} \in \mathbb{C}^{(N-1)\times 1}$ denotes the weight vector for the interference rejection, $\mathbf{U} = [\mathbf{u}_1, \ldots, \mathbf{u}_{N-1}]$ represents the

target interference signals, and $\mathbf{x}$ denotes the input signal, which includes the desired signal and the interference signal. All of these signal matrices, such as $\mathbf{U}$ and $\mathbf{x}$, can be reconstructed from the result of the CFAR detection algorithm, i.e., $u_i(k) = s(k-\tau_i)e^{j2\pi v_i k}$ and $\mathbf{u}_i = [u_i(0), \ldots, u_i(K-1)]^T$.

As our objective is to obtain $\boldsymbol{\alpha}$, the minimization problem can be rewritten as

$$\hat{\boldsymbol{\alpha}} = \arg\min_{\boldsymbol{\alpha}} ||\mathbf{x} - \mathbf{U}\boldsymbol{\alpha}||^2. \tag{48}$$

The minimization with respect to $\boldsymbol{\alpha}$ leads to the least-squares problem, and we have

$$\hat{\boldsymbol{\alpha}} = (\mathbf{U}^H\mathbf{U})^{-1}\mathbf{U}^H\mathbf{x}. \tag{49}$$

When the steering vector of interest is denoted by $\mathbf{b}_d$ and the steering vectors of the interferences are written as $\mathbf{B}_u = [\mathbf{b}_1, \ldots, \mathbf{b}_{N-1}]$, then the output of the target interference cancellation is

$$\tilde{\mathbf{c}}_d = \mathbf{B}\mathbf{w} = \mathbf{b}_d - \mathbf{B}_u\boldsymbol{\alpha}, \tag{50}$$

where $\mathbf{B} = [\mathbf{b}_d, \mathbf{B}_u]$ and $\mathbf{w} = [1, -\boldsymbol{\alpha}^T]^T$. Finally, $\tilde{\mathbf{c}}_d$ is the steering vector estimate of interest.

The target interference cancellation algorithm may be summarized as follows:

- ***Step 1***: *Compute the steering vector of interest* $\mathbf{b}_d$ *using the detection results.*
- ***Step 2***: *Determine the steering vectors of the target interferences* $\mathbf{B}_u$ *that may cause the performance degradation in DOA estimation.*
- ***Step 3***: *Derive the target signal of interest* $\mathbf{x}$ *and the target interference signals* $\mathbf{U}$ *based on the target detection results.*
- ***Step 4***: *Determine* $\boldsymbol{\alpha}$ *and* $\mathbf{w}$ *with* (49).
- ***Step 5***: *Compute the final steering vector estimate of* $\tilde{\mathbf{c}}_d$ *with* (50).

V. SIMULATIONS

In this section, we present the simulation results to verify the theoretical results. Note that, in all examples, a uniform circular array with M antennas and a radius of 1.5 m is considered. The complex envelope of FM radio can be generated by

$$s(k) = \exp\left(j2\pi\,\Delta f \sum_{k=0}^{K-1} m(k)\Delta t\right), \tag{51}$$

where Δf denotes the frequency deviation of 75 kHz, $m(k)$ is a sampled message signal, and Δt denotes a sampling period (i.e., $1/f_s$). A sampling frequency of 198.45 kHz is also used to generate the signals. Because the FM radio broadcasting supports stereo sound, the message signal $m(k)$ contains both a left (L) and a right signal (R). The message signal $m(k)$ can be modeled as

$$m(k) = 0.9(0.5(L+R) + 0.5(L-R)\sin(4\pi f_p k\Delta t) + 0.1\sin(2\pi f_p k\Delta t)), \tag{52}$$

where f_p denotes a pilot tone signal of 19 kHz.

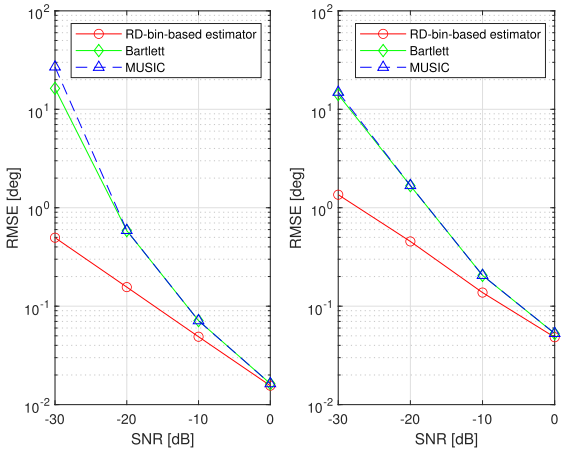

FIGURE 5. RMSEs of azimuth (left) and elevation (right) versus SNR with RD map-based DOA estimation of $L = 1$, Bartlett algorithm and MUSIC ($M = 8$, observation time: 1 sec).

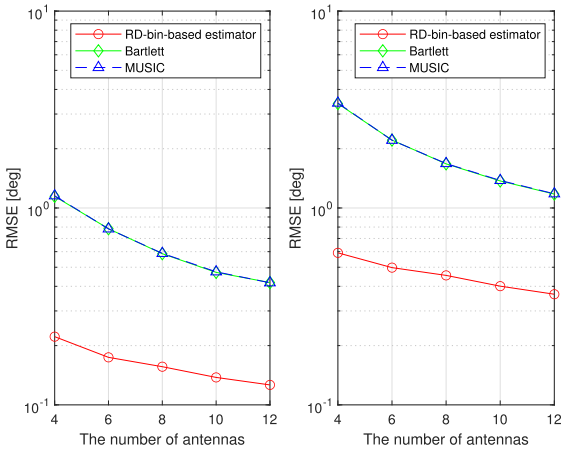

FIGURE 6. RMSEs of azimuth (left) and elevation (right) versus the number of antennas with RD map-based DOA estimation of $L = 1$, Bartlett algorithm and MUSIC (observation time: 1 sec, SNR: −20 dB).

We have not included the CRLB in all the simulation results. To the best of our knowledge, there is no previously published work that covers our signal model and scenario in which we consider the joint estimation of azimuth and elevation angle. There have been several related works (see [47]–[49]), but they only deal with a scenario assuming that the signal sources are located on a plane at z = 0 where the antennas are also placed (i.e., assuming that the elevation angle is equal to 90°).

Simulation 1: In this example, the root-mean-square error (RMSE) of the RD map-based DOA estimation with $L = 1$ is presented. To compare the estimation performance, we also consider the conventional Bartlett and the MUSIC algorithm. It is assumed that only one target signal is received and that the detection probability is equal to 1. We also assume that the measurements, such as the bistatic range and Doppler frequency of a target signal, are known. The target signal has an azimuth angle of 90° and an elevation angle of 70°. We conducted 500 Monte-Carlo simulations.

Figs. 5, 6, and 7 show the RMSEs of the RD map-based DOA estimation method, Bartlett algorithm and

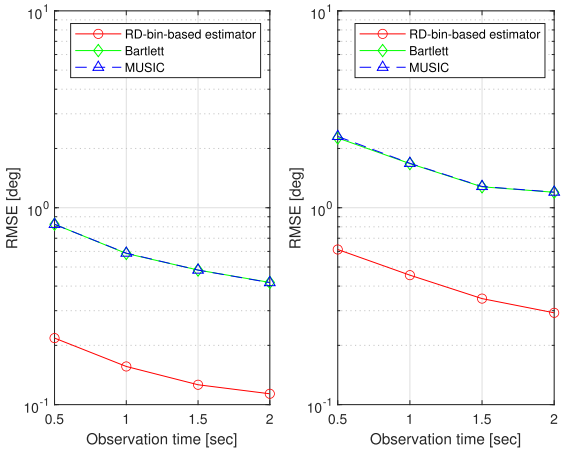

FIGURE 7. RMSEs of azimuth (left) and elevation (right) versus observation time with RD map-based DOA estimation of $L = 1$, Bartlett algorithm and MUSIC ($M = 8$, SNR: -20 dB).

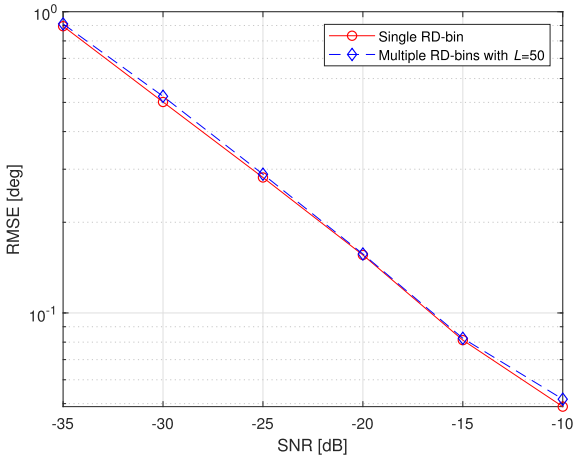

FIGURE 8. Root-mean-square errors of single RD-bin- and multiple RD-bin-based DOA estimation methods when the message is silent.

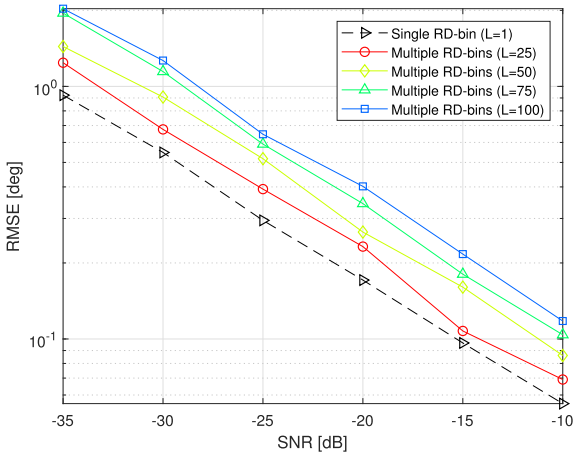

FIGURE 9. Root-mean-square errors of single RD-bin- and multiple RD-bin-based DOA estimation methods with the music message signal.

MUSIC algorithm. Several DOA estimation algorithms such as ESPRIT and Capon are not considered because these algorithms have almost the same estimation performance as that of Bartlett and MUSIC in the single-target environment.

Fig. 5 shows the RMSE versus the SNR of the target signal for the case of $M = 8$ and an observation time of 1 sec. The RD map-based DOA estimation with a single RD-bin shows a much lower estimation error than that of the Bartlett and MUSIC algorithms in cases of both azimuth and elevation estimations. In particular, with low SNRs ranging from -30 dB to -20 dB, the difference between the two methods is clearly seen.

Fig. 6 shows the RMSE versus the number of antennas. As in Fig. 5, the difference between RD-bin-based estimator and other algorithms can be observed. Fig. 7 also presents the RMSE versus the observation time. Because the RD map-based DOA estimation method properly uses the reference signal, the RD-bin-based estimator increases the processing gain of the target signal, and this leads to the performance improvement.

Simulation 2: Consider that the FM signal is generated from a silent signal (i.e., $L = R = 0$ in (52)). Then, the message signal has only a 19 kHz pilot tone, which is used for FM stereo. To simplify the simulations, we consider only the azimuth angle and assume $\theta = 90°$. In this case, the CAF has infinite range resolution, as in Fig. 2. Fig. 8 shows the RMSEs with $L = 1$ and $L = 50$. The difference between the two methods with single RD-bin and multiple RD-bins is not observed. As we derived in Section III, it is obvious that we have almost the same performance because of the theoretical output SNR.

Simulation 3: Fig. 9 shows the RMSE of RD map-based DOA estimation with $L = 1,\ 25,\ 50,\ 75$ and 100 when a music signal is used in the FM message. The CAF corresponding to this music message signal is shown in Fig. 4. As shown in Fig. 9, the RMSE of a method with multiple RD-bins is higher than that of the single RD-bin. We also can see that the RMSE increases as the number of RD-bins increases. These results show that the steering vector estimate includes more nonsignal components as L increases.

When a music signal is used for FM radio, it has a considerably wider instantaneous bandwidth. Therefore, the covariance matrix estimation performance with multiple bins is degraded by including several noise components. It is common to have much wider instantaneous bandwidth with FM radio than with AM radio. Therefore, we can conclude that it is more effective to use only one RD-bin for the DOA estimation in FM radio-based PBR.

Simulation 4: In this simulation, we consider the performance of the proposed algorithm for interference cancellation. We assume that $N = 5$ targets are lying on the same Doppler frequency dimension of -30 Hz and that the targets have a bistatic range of 50, 75, 100, 125, and 150 km. We also assume that the target signals have an SNR of -20 dB. Fig. 10 shows the magnitude of the weight vector $\mathbf{w}$ in (50). Each target has a weight vector for the removal of other target signals. If we consider target 1, the magnitude of the second entry of $\mathbf{w}$ has the most significant value. This means

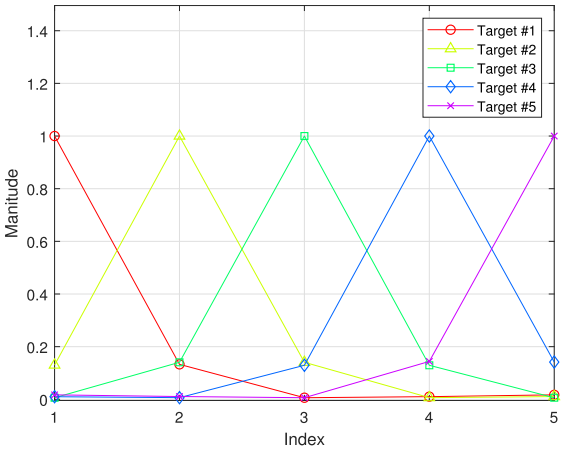

FIGURE 10. Magnitude of weight vector of w for the interference cancellation.

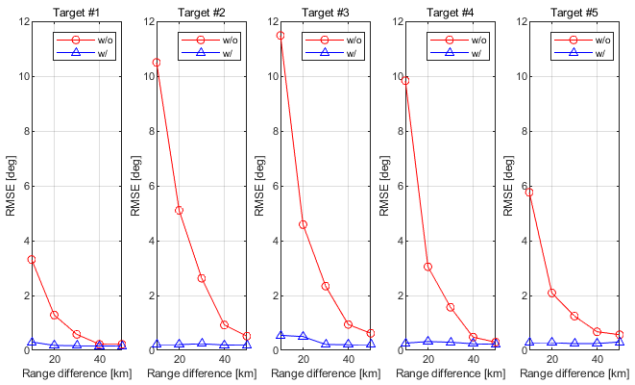

FIGURE 11. Root-mean-square error of multiple targets with and without the target interference cancellation algorithm.

that the adjacent target 2 component becomes the primary interference of target 1. In the case of target 2, target 1 and target 3 may be considered as the main interference signals. We can see that the weight vector is properly computed to represent the correlation between the adjacent targets for the interference cancellation.

Fig. 11 shows the RMSE of the multiple targets versus the range difference between the targets. If the bistatic range difference between the targets is denoted by ΔR, we set the bistatic range measurement of the ith target to $100 + (i-2)\Delta R$ km ($i = 0, 1, 2, 3, 4$). In this case, we can expect that, as the range difference increases, the estimation error will decrease. As we can see in Fig. 11, the RMSE without the target interference cancellation algorithm is significantly higher than that using the interference cancellation. Furthermore, the RMSE with the interference cancellation is not dramatically affected by the range difference. This result also shows that the proposed algorithm successfully removes the interference components.

VI. CONCLUSION

We examined the RD map-based DOA estimation method for FM radio-based PBR. In this regard, the output SNR of the steering vector estimate for the number of RD-bins was theoretically derived. As a result, we concluded that the output SNR does not change with the number of RD-bins for signals with narrow instantaneous bandwidths such as AM radio because the multiple RD-bins can include the signal components. However, the output SNR may be reduced for a signal having a relatively higher bandwidth than that of AM radio signals because the steering vector estimate may include the noise components. As FM radio has a wider bandwidth than AM radio, we concluded that it is reasonable to use the single RD-bin-based DOA estimation method for FM radio-based PBR.

We also suggested that other target signals can become interference signals in the presence of a plurality of targets, which may degrade the DOA estimation accuracy. The least-squares-based interference cancellation algorithm was proposed to solve this problem, and we showed that this proposed algorithm can mitigate the interference signals. We also presented the theoretical SNR loss of the target interference cancellation method. We verified from the analysis that the SNR loss of the proposed method could be ignored in FM radio-based PBR.

Unlike conventional algorithms such as Bartlett, Capon, and MUSIC, our proposed method is based on an RD map. Accordingly, we first need to obtain the RD map, and this leads to an increase in the computational complexity. The interference cancellation algorithm should be performed on each antenna, and this also produces additional computation. Therefore, in future works, we will study how to reduce the computational complexity of the proposed algorithms.

REFERENCES

[1] S. Paine, D. W. O'Hagan, M. Inggs, C. Schupbach, and U. Boniger, "Evaluating the performance of FM-based PCL radar in the presence of jamming," *IEEE Trans. Aerosp. Electron. Syst.*, vol. 55, no. 2, pp. 631–643, Apr. 2019.

[2] Y. Fu, X. Wan, X. Zhang, G. Fang, and J. Yi, "Side peak interference mitigation in FM-based passive radar via detection identification," *IEEE Trans. Aerosp. Electron. Syst.*, vol. 53, no. 2, pp. 778–788, Apr. 2017.

[3] B. Tuysuz, J. V. Urbina, and J. D. Mathews, "Effects of the equatorial electrojet on FM-based passive radar systems," *IEEE Trans. Geosci. Remote Sens.*, vol. 55, no. 7, pp. 4082–4088, Jul. 2017.

[4] A. Zaimbashi, "Multiband FM-based PBR system in presence of model mismatch," *Electron. Lett.*, vol. 52, no. 18, pp. 1563–1565, Sep. 2016.

[5] Y. Li, H. Ma, Y. Wu, L. Cheng, and D. Yu, "DOA estimation for echo signals and experimental results in the AM radio-based passive radar," *IEEE Access*, vol. 6, pp. 73316–73327, 2018.

[6] J. H. Huang, J. L. Garry, and G. E. Smith, "Array-based target localisation in ATSC DTV passive radar," *IET Radar, Sonar Navigat.*, vol. 13, no. 8, pp. 1295–1305, Aug. 2019.

[7] G. Bournaka, M. Ummenhofer, D. Cristallini, J. Palmer, and A. Summers, "Experimental study for transmitter imperfections in DVB-T based passive radar," *IEEE Trans. Aerosp. Electron. Syst.*, vol. 54, no. 3, pp. 1341–1354, Jun. 2018.

[8] S. Choi, D. Crouse, P. Willett, and S. Zhou, "Multistatic target tracking for passive radar in a DAB/DVB network: Initiation," *IEEE Trans. Aerosp. Electron. Syst.*, vol. 51, no. 3, pp. 2460–2469, Jul. 2015.

[9] H. Bolvardi, M. Derakhtia, and A. Sheiki, "Dynamic clutter suppression and multitarget detection in a DVB-T-Based passive radar," *IEEE Trans. Aerosp. Electron. Syst.*, vol. 53, no. 4, pp. 1812–1825, Aug. 2017.

[10] M. Edrich, F. Meyer, and A. Schroeder, "Design and performance evaluation of a mature FM/DAB/DVB-T multi-illuminator passive radar system," *IET Radar, Sonar Navigat.*, vol. 8, no. 2, pp. 114–122, Feb. 2014.

[11] B. Demissie, "Clutter cancellation in passive radar using GSM broadcast channels," *IET Radar, Sonar Navig.*, vol. 8, no. 7, pp. 787–796, 2014.
[12] R. Zemmari, B. Knoedler, and U. Nickel, "On angle estimation in GSM passive coherent location systems," in *Proc. 17th Int. Radar Symp. (IRS)*, Krakow, Poland, May 2016, pp. 1–5.
[13] F. Colone, T. Martelli, C. Bongioanni, D. Pastina, and P. Lombardo, "Wifi-based PCL for monitoring private airfields," *IEEE Aerosp. Electron. Syst. Mag.*, vol. 32, no. 2, pp. 22–29, Feb. 2017.
[14] M. Liu, J. Zhang, J. Tang, F. Jiang, P. Liu, F. Gong, and N. Zhao, "2-D DOA robust estimation of echo signals based on multiple satellites passive radar in the presence of alpha stable distribution noise," *IEEE Access*, vol. 7, pp. 16032–16042, 2019.
[15] N. J. Willis and H. D. Griffiths, *Advances in Bistatic Radar*. Rijeka, Croatia: SciTech, 2007.
[16] H. Kim and M. Viberg, "Two decades of array signal processing research," *IEEE Signal Process. Mag.*, vol. 13, no. 4, pp. 67–94, Jul. 1996.
[17] J. Capon, "High-resolution frequency-wavenumber spectrum analysis," *Proc. IEEE*, vol. 57, no. 8, pp. 1408–1418, Aug. 1969.
[18] R. Schmidt, "Multiple emitter location and signal parameter estimation," *IEEE Trans. Antennas Propag.* vol. 34, no. 3, pp. 276–280, Mar. 1986.
[19] A. J. Barabell, "Improving the resolution performance of eigenstructure-based direction-finding algorithms," in *Proc. ICASSP*, Boston, MA, USA, Apr. 1983, pp. 336–339.
[20] R. Roy, and T. Kailath, "ESPRIT-Estimation of signal parameters via rotational invariance techniques," *IEEE Trans. Acoust., Speech, Signal Process.*, vol. 37, no. 7, pp. 984–995, Jul. 1989.
[21] R. Kumaresan, and D. W. Tuft, "Estimating the angles of arrival of multiple plane waves," *IEEE Trans. Aerosp. Electron. Syst.*, vol. AES-19, no. 1, pp. 134–139, Jan. 1983.
[22] Z. Wang, W. Xie, Y. Zou, and Q. Wan, "DOA estimation using single or dual reception channels based on cyclostationarity," *IEEE Access*, vol. 7, pp. 54787–54795, 2019.
[23] J. Li, D. Li, D. Jiang, and X. Zhang, "Extended-aperture unitary root MUSIC-based DOA estimation for coprime array," *IEEE Commun. Lett.*, vol. 22, no. 4, pp. 752–755, Apr. 2018.
[24] A. Liu, X. Zhang, Q. Yang, and W. Deng, "Fast DOA estimation algorithms for sparse uniform linear array with multiple integer frequencies," *IEEE Access*, vol. 6, pp. 29952–29965, 2018.
[25] J. Shi, G. Hu, X. Zhang, F. Sun, and H. Zhou, "Sparsity-based two-dimensional DOA estimation for coprime array: From sum–difference coarray viewpoint," *IEEE Trans. Signal Process.*, vol. 65, no. 21, pp. 5591–5604, Nov. 2017.
[26] F. Wen, J. Shi, and Z. Zhang, "Joint 2D-DOD, 2D-DOA and polarization angles estimation for bistatic EMVS-MIMO radar via PARAFAC analysis," *IEEE Trans. Veh. Technol.*, vol. 69, no. 2, pp. 1626–1638, Feb. 2020, doi: 10.1109/TVT.2019.2957511.
[27] X. Wang, L. Wan, M. Huang, C. Shen, Z. Han, and T. Zhu, "Low-complexity channel estimation for circular and noncircular signals in virtual MIMO vehicle communication systems," *IEEE Trans. Veh. Technol.*, early access, Feb. 3, 2020, doi: 10.1109/TVT.2020.2970967.
[28] Y. Liu, X. Wan, H. Tang, J. Yi, Y. Cheng, and X. Zhang, "Digital television based passive bistatic radar system for drone detection," in *Proc. IEEE Radar Conf. (RadarConf)*, Seattle, WA, USA, May 2017, pp. 1493–1497.
[29] N. Del-Rey-Maestre, D. Mata-Moya, M. P. Jarabo-Amores, J. Rosado-Sanz, P. G.-D.-H. Del-Rey-Maestre, D. Mata-Moya, M.-P. Jarabo-Amores, J. Rosado-Sanz, and P. Gomez-del-Hoyo, "DoA estimation based on a ULA of commercial antennas in semi-urban passive radar scenario," in *Proc. Int. Conf. Control, Artif. Intell., Robot. Optim. (ICCAIRO)*, Prague, Czech Republic, May 2017, pp. 74–77.
[30] M.-C. Hua, C.-H. Hsu, and H.-C. Liu, "Joint TDOA-DOA localization scheme for passive coherent location systems," in *Proc. 8th Int. Symp. Commun. Syst., Netw. Digit. Signal Process. (CSNDSP)*, Poznan, Poland, Jul. 2012, pp. 1–4.
[31] G.-H. Park, D.-G. Kim, H. J. Kim, and H.-N. Kim, "Maximum-likelihood angle estimator for multi-channel FM-radio-based passive coherent location," *IET Radar, Sonar Navigat.*, vol. 12, no. 6, pp. 617–625, May 2018.
[32] F. Filippini, T. Martelli, F. Colone, and R. Cardinali, "Target DoA estimation in passive radar using non-uniform linear arrays and multiple frequency channels," in *Proc. IEEE Radar Conf. (RadarConf)*, Oklahoma City, OK, USA, Apr. 2018, pp. 1290–1295.
[33] F. Colone, G. De Leo, P. Paglione, C. Bongioanni, and P. Lombardo, "Direction of arrival estimation for multi-frequency FM-based passive bistatic radar," in *Proc. IEEE RadarCon (RADAR)*, Kansas City, MO, USA, May 2011, pp. 441–446.
[34] H. L. Van Trees, *Optimum Array Processing: Part IV of Detection, Estimationand Modulation Theory*. Hoboken, NJ, USA: Wiley, 2002.
[35] G. Bournaka, C. Schwark, D. Cristallini, and H. Kuschel, "Beam space transformation based direction of arrival estimation and auto calibration for a circular array in passive radar," in *Proc. IEEE Radar Conf. (RadarConf)*, Seattle, WA, USA, May 2017, pp. 745–748.
[36] L. Xiao-Yong, W. Jun, and W. Jue, "Robust direction of arrival estimate method in FM-based passive bistatic radar with a four-element Adcock antenna array," *IET Radar, Sonar Navigat.*, vol. 9, no. 4, pp. 392–400, Apr. 2015.
[37] J. Wang, H.-T. Wang, and Y. Zhao, "Direction finding in frequency-modulated-based passive bistatic radar with a four-element Adcock antenna array," *IET Radar, Sonar Navigat.*, vol. 5, no. 8, pp. 807–813, Oct. 2011.
[38] G. Bournaka, J. Heckenbach, A. Baruzzi, D. Cristallini, and H. Kuschel, "A two stage beamforming approach for low complexity CFAR detection and localization for passive radar," in *Proc. IEEE Radar Conf. (RadarConf)*, Philadelphia, PA, USA, May 2016, pp. 1–4.
[39] J. Palmer, "A signal processing scheme for a multichannel passive radar system," in *Proc. IEEE Int. Conf. Acoust., Speech Signal Process. (ICASSP)*, Brisbane, QLD, Australia, Apr. 2015, pp. 5575–5579.
[40] T.-T. Van Cao, "Sequential detection for passive radar part 1: The A-C DF-map detector," in *Proc. Int. Conf. Radar (RADAR)*, Brisbane, QLD, Australia, Aug. 2018, pp. 1–6.
[41] F. Colone, D. W. O'Hagan, P. Lombardo, and C. J. Baker, "A multistage processing algorithm for disturbance removal and target detection in passive bistatic radar," *IEEE Trans. Aerosp. Electron. Syst.*, vol. 45, no. 2, pp. 698–722, Apr. 2009.
[42] F. Colone, R. Cardinali, and P. Lombardo, "Cancellation of clutter and multipath in passive radar using a sequential approach," in *Proc. IEEE Conf. Radar*, Apr. 2006, pp. 393–399.
[43] F. Colone, C. Palmarini, T. Martelli, and E. Tilli, "Sliding extensive cancellation algorithm for disturbance removal in passive radar," *IEEE Trans. Aerosp. Electron. Syst.*, vol. 52, no. 3, pp. 1309–1326, Jun. 2016.
[44] B. C. Ng and C. M. S. See, "Sensor-array calibration using a maximum-likelihood approach," *IEEE Trans. Antennas Propag.*, vol. 44, no. 6, pp. 827–835, Jun. 1996.
[45] C. M. S. See and A. B. Gershman, "Direction-of-arrival estimation in partly calibrated subarray-based sensor arrays," *IEEE Trans. Signal Process.*, vol. 52, no. 2, pp. 329–338, Feb. 2004.
[46] H. Rohling, "Radar CFAR thresholding in clutter and multiple target situations," *IEEE Trans. Aerosp. Electron. Syst.*, vol. AES-19, no. 4, pp. 608–621, Jul. 1983.
[47] F. Bellili, S. Affes, and A. Stephenne, "On the lower performance bounds for DOA estimators from linearly-modulated signals," in *Proc. 25th Biennial Symp. Commun.*, Kingston, ON, Canada, May 2010, pp. 381–386.
[48] T. Basikolo, K. Ichige, and H. Arai, "A note on CRLB formulation for underdetermined DOA estimation in circularly configured planar arrays," *IEICE Electron. Express*, vol. 15, no. 6, 2018, Art. no. 20180193.
[49] B. R. Jackson, S. Rajan, B. J. Liao, and S. Wang, "Direction of arrival estimation using directive antennas in uniform circular arrays," *IEEE Trans. Antennas Propag.*, vol. 63, no. 2, pp. 736–747, Feb. 2015.

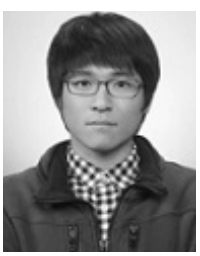

GEUN-HO PARK received the B.S., M.S., and Ph.D. degrees in electronic and electrical engineering from Pusan National University (PNU), Busan, South Korea, in 2013, 2015, and 2020, respectively. Since 2020, he has been a Researcher with the Department of Electrical and Computer Engineering, Pusan National University. His main research interests include digital signal processing, array signal processing, radar signal processing, deep neural networks (DNNs), reinforcement learning, and electronic warfare (EW) systems.

YOUNG-KWANG SEO received the B.S., M.S., and Ph.D. degrees in electronic and electrical engineering from Pusan National University (PNU), Busan, South Korea, in 2012, 2014, and 2019, respectively. From 2019 to March 2020, he was a Researcher with the Department of Electrical and Computer Engineering, Pusan National University. Since March 2020, he has been a Senior Researcher with the Hanwha Systems, South Korea. His main research interests include radar signal processing, sonar signal processing, and machine learning (ML).

HYOUNG-NAM KIM (Member, IEEE) received the B.S., M.S., and Ph.D. degrees in Electronic and Electrical Engineering from the Pohang University of Science and Technology, Pohang, South Korea, in 1993, 1995, and 2000, respectively. From 2000 to 2003, he was with the Electronics and Telecommunications Research Institute, Daejeon, South Korea, where he was developing advanced transmission and reception technology for terrestrial digital television. In 2003, he joined the Faculty of the Department of Electronics Engineering, Pusan National University, Busan, South Korea, where he is currently a full-time Professor. From 2009 to 2010, he was a Visiting Scholar with the Department of Biomedical Engineering, Johns Hopkins School of Medicine. From 2015 to 2016, he was a Visiting Professor with the School of Electronics and Computer Engineering, University of Southampton, U.K. His research interests include digital signal processing, radar/sonar signal processing, adaptive filtering, and biomedical signal processing, in particular, signal processing for digital communications, electronic warfare support systems, and brain–computer interfaces. He is a member of IEEK and KICS.